Kinetics and Catalysis, Vol. 46, No. 5, 2005, pp. 752–757. Translated from Kinetika i Kataliz, Vol. 46, No. 5, 2005, pp. 795–800.

Self-Propagating Synthesis of Supported Oxide Catalysts for Deep Oxidation of CO and Hydrocarbons

U. F. Zav'yalova*, V. F. Tret'yakov*, T. N. Burdeinaya*, V. V. Lunin*, N. B. Shitova, N. D. Ryzhova**, A. N. Shmakov***, A. I. Nizovskii***, and P. G. Tsyrul'nikov****

** Topchiev Institute of Petrochemical Synthesis, Russian Academy of Sciences, Moscow, 117912 Russia*

*** Institute of Hydrocarbon Conversion, Siberian Division, Russian Academy of Sciences, Omsk, Russia*

**** Boreskov Institute of Catalysis, Siberian Division, Russian Academy of Sciences, Novosibirsk, 630090 Russia*

Received October 15, 2004

Abstract—The surface self-propagating thermal synthesis (SSTS) of supported oxide catalysts is reported, which is a new modification of self-propagating high-temperature synthesis. The propagation of the combustion front on a variety of supports differing in nature and shape is studied. A group of catalysts based on simple and mixed oxides of cobalt, copper, and manganese are prepared by SSTS, and their physicochemical properties are determined. The dependence of synthesis parameters on catalyst preparation conditions is studied. The activity of the resulting catalysts is estimated in deep CO and methane oxidations as model reactions.

In recent years, intensive research has been aimed at new methods for catalyst preparation, since the efficiency of an industrial catalytic process depends considerably on the method by which the catalyst was prepared. The rapidly developing unconventional methods of catalyst preparation include the pyrolysis of volatile compounds of metals on a hot surface, the decomposition of colloidal dispersions of salts of higher acids in alcohol on a support, metal electrodeposition, synthesis under supercritical conditions, mechanochemical synthesis, plasma chemical methods, self-propagating high-temperature synthesis (SHS), etc. [1].

The SHS method is distinguished by a low energy consumption and a high synthesis rate and provides the possibility of converting inorganic materials into final products in one step, utilizing the chemical energy of the reaction. For these reasons, SHS is widely used in obtaining various materials [2, 3]. However, as applied to catalyst preparation, this method suffers from limitations arising from the fact that very high temperatures develop during the synthesis and it is difficult to control the process in the extremal regime. In this method, catalysts are obtained from a mixture of fine powders of precursors (metals, metal oxides, etc.) that can react, evolving a large amount of energy. After the exothermic reaction is initiated, a heat wave having a temperature of 1000–2000°C travels throughout the volume of the batch to yield a catalyst monolith with a small specific surface area of ~0.01–4.0 m^2/g [4–6]. As a rule, catalysts prepared by SHS are less active than their counterparts prepared by conventional methods such as extrusion and the supporting of an active component followed by heat treatment. Catalysts obtained by SHS are most widely employed in the high-temperature cracking of hydrocarbons [6].

The basic approaches to the improvement of this method are reducing the proportion and particle size of the active components. This is achieved by varying synthesis conditions while controlling the main process parameters, namely, synthetic temperature and the velocity of the combustion front. A modification of the SHS method is surface self-propagating thermal synthesis (SSTS), which is used to obtain oxide catalysts on chemically and geometrically diverse supports [7].

The SSTS method is based on the self-propagating combustion of precursors of the active components of the catalyst and utilizes the energy of exothermic reactions. In this method, a support is impregnated with chemicals that can react with one another or with atmospheric oxygen to release an amount of energy sufficient to sustain combustion and to compensate for the heat dissipated into the environment. The highest heat wave temperature in the SSTS method (600–700°C) is much lower than the same temperature in the SHS method, preventing the active component from agglomeration on the support. SSTS allows one to use chemically and geometrically diverse supports (e.g., pellets, monoliths, and stripes). After a short-term initiation of the exothermic reaction, a nonflame combustion front travels throughout the sample to yield an active component uniformly distributed over the support and tightly bound to the support surface. Such synthesis can be carried out either on the surface of a glass-fiber stripe or a metal support or in the pores of a high-porosity material.

The purpose of this work is to establish fundamental laws of self-propagating thermal synthesis and to optimize the process so as to obtain oxide catalysts for deep CO and methane oxidation (model reactions) on supports varying in nature and shape.

0023-1584/05/4605-0752 © 2005 MAIK "Nauka/Interperiodica"

Table 1. Properties of catalyst supports

No.	Support	Dimensions, mm	S_{sp}, m^2/g	Pore radius, μm	Water-filled pore volume, cm^3/g
1	Glass cloth	$60 \times 5.0 \times 1.0$	1.2	<1 μm	0.50
2	Reinforced Ti–Si alloy	$60 \times 5.0 \times 1.0$	0.1	–	0.08
3	Reinforced Ni–Al–Si alloy	$60 \times 5.0 \times 1.0$	0.1	–	0.08
4	Porous steel	$60 \times 5.0 \times 2.0$	0.1	4–6	0.05
5	Porous Ti	$60 \times 5.0 \times 2.0$	0.1	3–5	0.05
6	γ-Al_2O_3	Size fraction 0.4–0.8	200.0	–	0.68

EXPERIMENTAL

Catalysts were prepared using the transition-metal acetate and nitrate crystalline hydrates $Co(CH_3COO)_2 \cdot 4H_2O$, $Cu(CH_3COO)_2 \cdot H_2O$, $Mn(CH_3COO)_2 \cdot 4H_2O$, $Co(NO_3)_2 \cdot 6H_2O$, and $Cu(NO_3)_2 \cdot 3H_2O$ (99.0%, Merck). Pure-grade carbamide, $CO(NH_2)_2$, was used as a calorific component. The self-propagating thermal synthesis was conducted on glass-fiber and metal stripes and in a γ-Al_2O granular bed (Table 1). The supports, preliminarily calcined at 600°C, were impregnated with precursor solutions by the incipient-wetness method and were dried in air at 100°C. The reaction was initiated for 5 s with a nichrome coil heated to ≥500°C. Heat wave temperature was measured with a fast chromel–alumel thermocouple. Combustion front velocity was calculated as the ratio of the sample length to the wave propagation time. The self-propagating thermal synthesis of catalysts on granular γ-Al_2O_3 was carried out in a quartz reactor (Fig. 1).

The synthesis products were identified by X-ray powder diffraction on a DRON-3 diffractometer using monochromated CuK_α radiation in a 2θ range of 20°–60°. Active component content was determined by atomic absorption spectroscopy. The specific surface area of catalysts was determined by the BET method from thermal argon desorption data using a Sorpty (Carlo Erba, Italy) instrument. The thermal analysis of precursors and catalysts was performed on a DTG-60 (Shimadzu, Japan) thermoanalytical system.

The mechanism of self-propagating thermal synthesis was studied by *in situ* time-resolved diffractometry on an anomalous scattering station designed at the Siberian Center for Synchrotron Studies (Budker Institute of Nuclear Physics, Siberian Division, Russian Academy of Sciences).

Microgrpahs of the catalysts were obtained using an LEO-32 (Germany) thermionic-emission scanning electron microscope operating at an accelerating voltage of 20 kV.

The catalysts were tested in the deep oxidation of CO and methane in a circulating flow reactor under gradientless conditions. Prior to activity tests, the catalysts were conditioned in the reaction medium until constant conversion. Catalytic activity was characterized by a CO or methane oxidation rate (w, cm^3 (g Cat)$^{-1}$ s^{-1}). Methane oxidation tests were performed at 500°C, an initial methane concentration of 0.5 vol %, and a methane conversion of X = 50%. CO oxidation tests were conducted at 150°C, an initial CO concentration of 1.0 vol %, and X = 50%.

RESULTS AND DISCUSSION

Self-Propagating Thermal Synthesis of the Active Components of Catalysts

Table 2 presents the thermochemical equations of the reactions taking place in the self-propagating synthesis of oxides on the supports. Three types of reaction were used in the synthesis, namely, the oxidation of an acetate with atmospheric oxygen (reactions (I)–(III)), the redox reaction between a metal acetate and a metal nitrate in the presence of oxygen (reactions (IV)–(VI)), and the reaction between copper nitrate and carbamide in

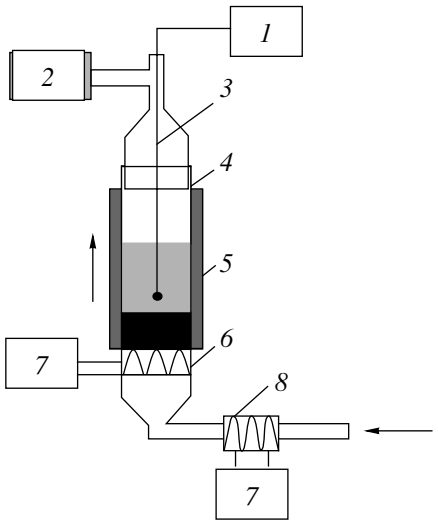

Fig. 1. Reactor for the SSTS of oxide catalyst on porous granular supports: (*1*) temperature controller, (*2*) adsorbent-filled trap, (*3*) fast thermocouple, (*4*) quartz reactor, (*5*) asbestos jacket, (*6*) nichrome coil for initiating the exothermic reaction, (*7*) adjustable voltage transformer, and (*8*) nichrome coil for preheating the oxidizing gas.

Table 2. Reactions occurring in SSTS and their enthalpies

Reaction		$\Delta H°$(298 K), kJ/mol [8, 9]
$3Co(CH_3COO)_2(s) + 12.5O_2(g) = Co_3O_4(s) + 12CO_2(g) + 9H_2O(g)$	(I)	–4836.3
$Cu(CH_3COO)_2(s) + 4O_2(g) = CuO(s) + 4CO_2(g) + 3H_2O(g)$	(II)	–2038.6
$3Mn(CH_3COO)_2(s) + 12.5O_2(g) = Mn_3O_4(s) + 12CO_2(g) + 9H_2O(g)$	(III)	–4862.5
$3Co(CH_3COO)_2(s) + 3Co(NO_3)_2(s) + 11.5O_2(g) = 2Co_3O_4(s) + 12CO_2(g) + 9H_2O(g) + 6NO_2(g)$	(IV)	–2133.4
$Cu(CH_3COO)_2(s) + Cu(NO_3)_2(s) + 3.5O_2(g) = 2CuO(s) + 4CO_2(g) + 3H_2O(g) + 2NO_2(g)$	(V)	–915.8
$3Mn(CH_3COO)_2(s) + 3Mn(NO_3)_2(s) + 11.5O_2(g) = 2Mn_3O_4(s) + 12CO_2(g) + 9H_2O(g) + 6NO_2(g)$	(VI)	–2167.2
$Cu(NO_3)_2(s) + CO(NH_2)_2(s) + 3O_2(g) = CuO(s) + CO_2(g) + 2H_2O(g) + 4NO_2(g)$	(VII)	–152.1

the presence of oxygen (reaction (VII)). These exothermic reactions yield a transition metal oxide in 1–10 min. The thermal front temperature does not exceed 450°C because of the considerable heat transfer from the surface.

The parameters of self-propagating combustion and the physicochemical and catalytic properties of the reaction product are known to depend considerably on the oxidizer-to-reducer ratio in the original mixture [10]. In order to see how the mechanism of the formation of catalytically active phases depends on this ratio, we carried out a comparative study of the syntheses involving the first two types of reaction.

By way of example, we present, in Fig. 2, time-resolved *in situ* X-ray diffraction data illustrating the formation of the active phase in the SSTS of the Co_3O_4/glass cloth catalyst. Diffraction patterns were taken every 5 s over 250 s during the propagation of the cobalt acetate combustion front. The self-propagating combustion of cobalt acetate according to reaction (I) (Table 2) is a two-step process. The first step yields CoO as an intermediate product 60 s after the initiation of combustion. The spinel oxide Co_3O_4, which is the main reaction product, results from the subsequent oxidation of CoO. The macromechanism of the formation of the active phase in the cobalt acetate–air combustion front can schematically be represented as

$$3Co(CH_3COO)_2 + 12O_2 = 3CoO + 12CO_2 + 9H_2O, \quad \text{(Ia)}$$

$$3CoO + 0.5O_2 = Co_3O_4. \quad \text{(Ib)}$$

The self-propagating combustion of a stoichiometric mixture of cobalt nitrate and cobalt acetate (Table 2, reaction (IV)) is a single-step process yielding no intermediate phases. In this case, oxidation is due to not only atmospheric oxygen but also the nitrate ions present in the original mixture. As a consequence, cobalt oxidation begins immediately after initiation, resulting in a finer Co_3O_4 phase. According to scanning electron microscopy data (Fig. 3), the self-propagating combustion of the equimolar mixture of cobalt acetate and cobalt nitrate on glass cloth (S_{sp} = 1.2 m^2/g) results

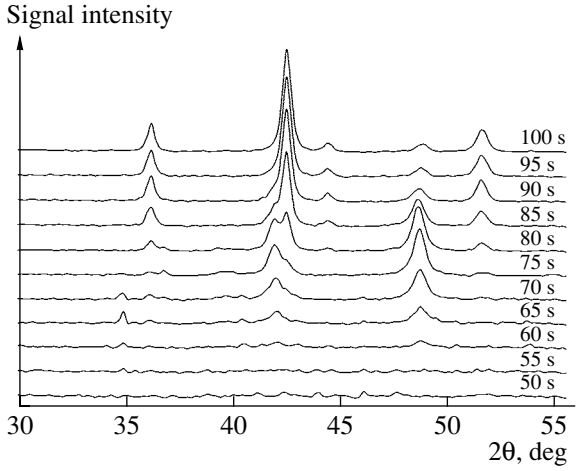

Fig. 2. X-ray diffraction patterns recorded during the SSTS of the Co_3O_4/glass cloth catalyst. The salt content is 40.0 wt %. The time elapsed from the synthesis initiation point is indicated for each diffraction pattern.

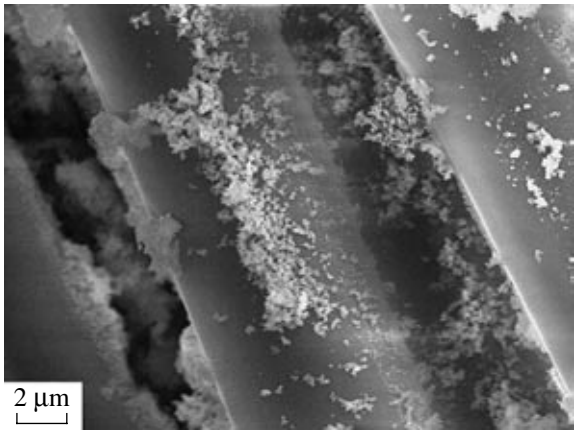

Fig. 3. Micrographs of the 10.0% Co_3O_4/glass cloth catalyst prepared by SSTS from a $Co(Ac)_2/Co(NO_3)_2$ = 1 : 1 mixture.

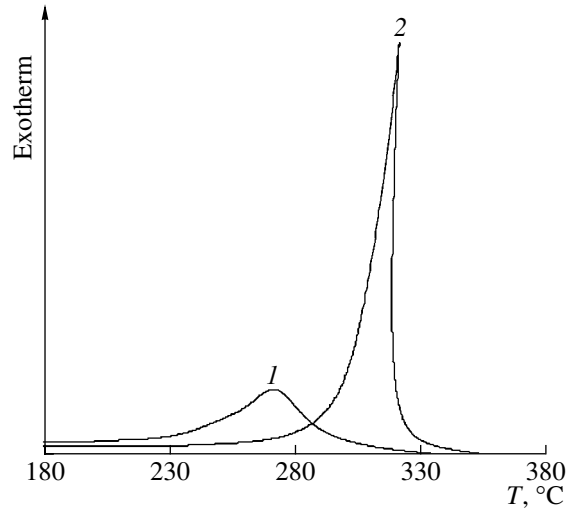

Fig. 4. DTA curves for the air oxidation of (*1*) an equimolar mixture of copper nitrate and acetate and (*2*) pure cobalt acetate supported on γ-Al_2O_3. The salt content is 15.0 wt %.

in uniformly distributed Co_3O_4 with a particle size below 0.1 μm.

Thermoanalytical data for the oxidation of γ-Al_2O_3-supported cobalt salts in air at various oxidizer-to-reducer ratios are presented in Fig. 4. For the equimolar mixture of cobalt acetate and cobalt nitrate (curve *1*), the temperature range of reaction is shifted to lower temperatures relative to that for pure cobalt acetate (curve *2*). It is likely that, in this mixture, nitrate decomposition and acetate combustion are accompanied by a redox reaction between the anions. The maximum combustion front temperature (T_{max}) is lower in the mixture than in pure acetate. Conversely, the synthesis rate (V) is higher in the mixture than in pure acetate because of the absence of limitations associated with the diffusion of the oxidizer to salt particles.

Dependence of Synthesis Parameters on Catalyst Preparation Conditions

Figure 5 presents thermoanalytical data for the air oxidation of cobalt, copper, and manganese acetates. The heat of reaction for these salts decreases in the order $Q_{MnAc_2} > Q_{CoAc_2} > Q_{CuAc_2}$. Temperature curves for the thermal front moving in the support bed during the synthesis of oxide catalysts from γ-Al_2O_3-supported cobalt, copper, and manganese acetates are plotted in Fig. 6. The variation of the maximum temperature of the heat wave (Fig. 6) is consistent with thermoanalytical data (Fig. 5) and with the heats of air oxidation of the metal acetates (reactions (I)–(III)): $T_{Mn_3O_4} > T_{Co_3O_4} > T_{CuO}$. The order of propagation velocities of solid-phase combustion is different: $V_{Co_3O_4} < V_{Mn_3O_4} < V_{CuO}$. This order is consistent with the temperature ranges in which

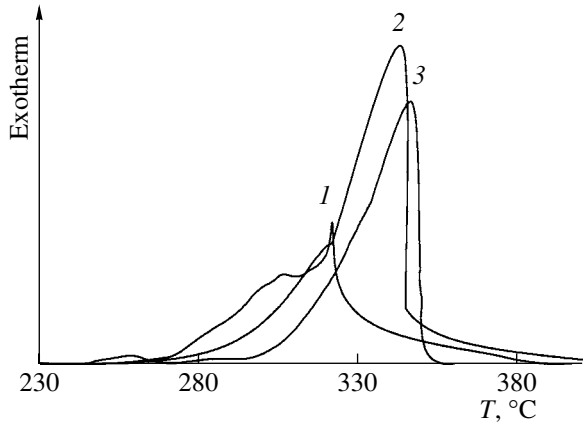

Fig. 5. DTA curves for the air oxidation of (*1*) $CuAc_2 \cdot H_2O$, (*2*) $MnAc_2 \cdot 4H_2O$, and (*3*) $CoAc_2 \cdot 4H_2O$.

cobalt, copper, and manganese acetates oxidize in air (Fig. 5). It is possible that the propagation velocity of solid-phase combustion is affected by those of the oxide phases forming at the combustion front that are active in deep oxidation reactions and can, therefore, catalyze further oxidation. That is, autocatalysis is possible.

To study the dependence of SSTS parameters on active component content, we measured the temperature and velocity of the thermal front for various supports loaded with 1.0 to 25.0 wt % metal acetate. The heat wave temperature increases with increasing percentage of supported salt for all supports and precursors examined. This effect is due to the increase in the concentration of reacting particles on a unit area of the support and, accordingly, in the heat released in a unit time. Conversely, the velocity of the combustion front falls with increasing oxide content, apparently because of

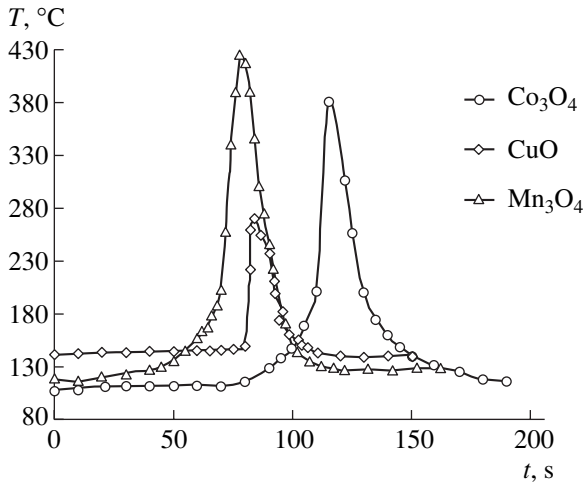

Fig. 6. Temperature curves characterizing the motion of the thermal front in γ-Al_2O_3 beds supporting Cu, Mn, and Co acetates. The oxide content is 5.0 wt %.

Table 3. Synthesis parameters and methane oxidation activity data for glass-cloth-supported simple and mixed oxides of Co, Cu, and Mn (the oxide content of the catalysts is 5.0 wt %)

Active component	T_{max}, °C	V, mm/s	$w \times 10^2$, $cm^3\ g^{-1}\ s^{-1}$
Co_3O_4	380	0.9	0.6
CuO	270	1.3	0.4
Mn_3O_4	420	1.2	0.3
$CuMnO_x$	345	1.3	0.1
$CoMnO_x$	400	1.0	0.2
$CuCo_{0.5}O_x$	305	1.1	2.1
$CuCoO_x$	325	1.1	1.8
$CuCo_2O_x$	350	1.1	3.7

Table 4. Effect of the support on the deep methane oxidation activity of catalysts

No.	Support	S_{sp}, m^2/g	$w \times 10^2$, $cm^3\ g^{-1}\ s^{-1}$
1	Glass cloth	5.4	0.6
2	Reinforced Ti–Si alloy	0.1	0.3
3	Reinforced Ni–Al–Si alloy	0.1	0.4
4	Porous steel	0.1	0.2
5	Porous Ti	0.1	0.2
6	γ-Al_2O_3	238.0	1.8

the increasingly hindered access of oxygen to the reacting molecules. In all cases, the velocity of the combustion front increases as the rate of feeding of pure or atmospheric oxygen to the supported precursor is raised. Therefore, SSTS is controlled to a considerable extent by the diffusion of the gaseous reactant to the salt particles.

It was demonstrated in an earlier study [7] that, besides the oxidizer supply rate and the percentage of the precursors of active components, there are other significant factors in the temperature and rate of self-propagating combustion: preheating temperature, the residual moisture content of the specimen, and the nature of the addition that sustains SSTS and is not an active component.

Dependence of the Catalytic Properties of the Specimens Synthesized on the Nature of the Support and Precursor

Table 3 lists synthesis parameters for catalysts based on simple and mixed oxides of cobalt, copper, and manganese prepared by SSTS and data characterizing the activity of these catalysts in the deep oxidation of methane. Of the simple oxides supported on glass cloth, Co_3O_4 is the most active. Of the cobalt–manganese, copper–cobalt, and copper–manganese systems, the copper–cobalt system is the most active. Its activity is higher than the activity of Co_3O_4, the most active simple oxide. Apparently, the increased catalytic activity of the copper–cobalt catalysts is due to the synergistic effect of their components. This effect is known from the literature [11] and, as indicated by X-ray diffraction data, arises from the formation of $CuCo_2O_4$–Co_3O_4, a nonstoichiometric solid solution with a spinel structure.

Table 4 lists data illustrating the effect of the support material on the specific surface area and activity of the 5.0% Co_3O_4 catalysts prepared by SSTS from cobalt acetate. The most active specimen is obtained with γ-Al_2O_3, which has the largest specific surface area.

In Table 5, we present data illustrating the effect of the precursor on the synthesis parameters and on the activity of the 5.0% Co_3O_4/γ-Al_2O_3 catalyst in the deep oxidation of CO and methane. Adding an equimolar amount of copper nitrate to copper acetate reduces the maximum temperature of the combustion front, because the decomposition of copper nitrate is endothermic and, as is demonstrated above (Fig. 4), the redox reaction between the anions produces less heat than the air oxidation of pure cobalt acetate. The activity of the

Table 5. Effect of the precursor on the synthesis parameters and the CO and methane oxidation activities of the 5.0% Co_3O_4/γ-Al_2O_3 catalyst

Preparation method	Precursor	T_{max}, °C	V, mm/s	$w \times 10^2$, $cm^3\ g^{-1}\ s^{-1}$	
				CH_4	CO
SSTS	$CoAc_2$	350	0.3	1.8	55.0
SSTS	$Co(Ac)_2/Co(NO_3)_2 = 1:1$	295	0.4	4.2	137.0
SSTS	$Co(NO_3)_2/CO(NH_2)_2 = 1:1$	260	0.2	0.9	30.0
Calcination*	$Co(NO_3)_2$	350	–	1.0	35.0

* The calcination time is 4 h.

resulting catalyst is four times higher than the activity of the specimen with the same composition obtained by a conventional method (calcination in a muffle furnace at 350°C for 4 h) [12]. At the same time, the catalyst resulting from copper nitrate in the presence of carbamide as a calorific component is less active than the catalyst prepared from copper acetate, even though carbamide decreases the synthesis temperature. According to X-ray diffraction data, this is due to the formation of CoO as a reaction product, which is less active in deep oxidation than the spinel oxide Co_3O_4.

CONCLUSIONS

A quick and environmentally friendly method involving the self-propagating combustion of active component precursors has been suggested for preparing oxide catalysts on supports varying in nature and shape. According to *in situ* time-resolved X-ray diffraction data, the mechanism of the formation of active phases at the combustion front depends on the oxidizer-to-reducer ratio in the original mixture. The combustion of cobalt acetate on the support surface is a two-step process yielding CoO as an intermediate. By contrast, the synthesis of fine Co_3O_4 by the redox reaction between cobalt acetate and nitrate proceeds at a higher rate and consists of a single step.

The temperature and velocity of the combustion front, which are the basic synthesis parameters, depend on the nature and proportions of the active component precursors, the oxidizer supply rate, the residual moisture content of the specimen, the temperature to which the specimen is preheated, and the nature of the calorific agent (which is not an active component and is added for sustaining the self-propagating synthesis). The catalysts prepared by SSTS are more active in CO and CH_4 oxidation than their analogues prepared by conventional methods.

ACKNOWLEDGMENTS

This work was supported in part by Haldor Topsøe Co.

REFERENCES

1. Pakhomov, N.A. and Buyanov, R.A., *Tezisy dokladov V Rossiskoi konferentsii po nauchnym osnovam prigotovleniya i tekhnologii katalizatorov* (Proc. V Russian Conf. on the Scientific Foundations of Catalyst Preparation and Technology), Novosibirsk, 2004, p. 7.
2. *Khimiya sinteza szhiganiem* (Chemistry of Combustion Synthesis), Koidzumi, M., Ed., Moscow: Mir, 1998, p. 11.
3. Merzhanov, A.G., *Protsessy goreniya i sintez materialov* (Combustion and Synthesis of Materials), Chernogolovka: Inst. of Structural Macrokinetics, 1998.
4. Xanthopoulou, G. and Vekinis, G., *Appl. Catal., B*, 1998, vol. 19, p. 37.
5. Colomer, M.T., Fumo, D.A., Jurado, J.R., and Segadaes, A.M., *J. Mater. Chem.*, 1999, vol. 9, p. 2505.
6. Xanthopoulou, G. and Vekinis, G., *Appl. Catal., A*, 2000, vol. 199, no. 2, p. 227.
7. RF Patent 2234979, 2004.
8. Knunyants, I.L., *Khimicheskaya entsiklopediya* (Encyclopedia of Chemistry), Moscow: Sovetskaya Entsiklopediya, 1990.
9. Turova, N.Ya., *Neorganicheskaya khimiya v tablitsakh. Uchebnoe posobie* (Inorganic Chemistry in Tables: A Textbook), Moscow: CheRo, 2002.
10. Tukhtaev, R.K., Boldyrev, V.V., Gavrilov, A.I., and Larionov, S.V., *J. Therm. Anal.*, 2003, vol. 71, no. 3, p. 841.
11. USSR Inventor's Certificate no. 844038, *Byull. Izobret.*, 1981.
12. Liotta, L.F., Pantaleo, G., Macaluso, A., Di Carlo, G., and Deganello, G., *Appl. Catal., A*, 2003, vol. 245, p. 167.